LONG-TERM STABILITY OF HIGH-LEVEL NUCLEAR WASTE CONTAINER MATERIALS: I - THERMAL STABILITY OF ALLOY 825

Prepared for

Nuclear Regulatory Commission
Contract NRC-02-88-005

Prepared by

Center for Nuclear Waste Regulatory Analyses
San Antonio, Texas

February 1993

CNWRA 93-003

LONG-TERM STABILITY OF HIGH-LEVEL NUCLEAR WASTE CONTAINER MATERIALS: I — THERMAL STABILITY OF ALLOY 825

Prepared for

Nuclear Regulatory Commission
Contract NRC-02-88-005

Prepared by

Gustavo Cragnolino
Narasi Sridhar

Center for Nuclear Waste Regulatory Analyses
San Antonio, Texas

February 1993

PREVIOUS REPORTS IN SERIES

Number	Name	Date Issued
CNWRA 91-004	A Review of Localized Corrosion of High-Level Nuclear Waste Container Materials — I	April 1991
CNWRA 91-008	Hydrogen Absorption and Embrittlement of Candidate Container Materials	June 1991
CNWRA 92-021	A Review of Stress Corrosion Cracking of High-Level Nuclear Waste Container Materials — I	August 1992

ABSTRACT

This report describes the initial activities conducted in the Integrated Waste Package Experiments (IWPE) program to study long-term thermal stability of the metallurgical phases present in candidate high-level waste (HLW) container materials selected for the proposed repository at Yucca Mountain. This report focusses on the effect of heat treatment temperatures (600 to 800°C) and times (0.1 to 15 hours) on the grain boundary precipitation and sensitization of alloy 825. Sensitization was evaluated by measuring corrosion rates in boiling 65 percent nitric acid solution according to ASTM A-262-90, Standard Practice C. It was found that the mill-annealed material, in spite of the low carbon content (0.01 weight percent), which is a characteristic of new production methods, became sensitized after 15 hours treatment at temperatures ranging from 650 to 750°C. The degree of sensitization was enhanced by solution annealing (1200°C for 10 minutes) prior to the sensitization heat treatments. A time-temperature-sensitization diagram was drawn for both metallurgical conditions. The sensitization process was found to be strongly dependent on temperature, with an apparent activation energy of 292 kJ/mole, which indicates that heat treatment extended for more than 18 years will be necessary to induce sensitization at 400°C. Continuation of these studies in the 400 to 600°C range using cold-worked samples is recommended to reliably predict the behavior of alloy 825 at the temperatures prevailing under repository conditions.

CONTENTS

FIGURES

TABLES

ACKNOWLEDGMENTS

This report was prepared to document work performed by the Center for Nuclear Waste Regulatory Analyses (CNWRA) for the U.S. Nuclear Regulatory Commission (NRC) under Contract No. NRC-02-88-005. The activities reported here were performed on behalf of the NRC Office of Nuclear Regulatory Research, Division of Regulatory Applications, Dr. Michael McNeil, Project Officer. The report is an independent product of the CNWRA and does not necessarily reflect the views or regulatory position of the NRC.

The authors gratefully acknowledge the contribution of Walt Machowski, Donald Pile, and James Spencer to this work, and the technical review of Hersh Manaktala. Appreciation is due to Bonnie Garcia and Curtis Gray for their assistance in the preparation of this report.

1 INTRODUCTION

The U.S. Nuclear Regulatory Commission (NRC) regulation 10 CFR 60.113 requires waste packages to provide substantially complete containment of radionuclides for a minimum period of 300 to 1000 years. Arising from this requirement is the need for the U.S. Department of Energy (DOE) to demonstrate acceptable long-term performance of waste packages through proper selection, design, testing, and analyses. In order to evaluate DOE's resolution of these technical issues, the NRC must develop an understanding of the important factors that affect long-term performance of waste package materials and components. Other considerations are the suitability and limitations of various test methods used to demonstrate performance, as well as the influence of factors not addressed by DOE, that may affect the performance of waste packages. The Integrated Waste Package Experiments (IWPE) research program at the Center for Nuclear Waste Regulatory Analyses (CNWRA) supports the NRC in attaining this understanding through a program plan divided into five interrelated tasks:

Task 1:	Corrosion
Task 2:	Stress Corrosion Cracking
Task 3:	Materials Stability
Task 4:	Microbiologically Influenced Corrosion
Task 5:	Other Degradation Modes

The present report describes the initial activities conducted under Task 3. The main objective in this task is to study the long-term thermal stability of the metallurgical phases present in the candidate high-level waste (HLW) container materials. In particular, this report is focused on the evaluation of the effect of certain combinations of heat treatment temperatures and times on the grain boundary precipitation and sensitization of alloy 825. This alloy is one of the three candidate container materials among the class of the austenitic Fe-Cr-Ni-Mo alloys originally selected by DOE for the proposed repository site at Yucca Mountain. Together with types 304L and 316L stainless steels, alloy 825 was chosen for the single-shell, thin-walled container design included in the Site Characterization Plan (McCright, 1988). It is currently being considered as one of the prime candidates for that design (McCright, 1991), as well as for the inner containment barrier of the double-shell container under evaluation in the Advanced Conceptual Design phase of the Yucca Mountain Project (Short et al., 1991; Stahl, 1992).

The range of heat treatment temperatures covered in the present study (600 to 800°C) is well beyond the range expected under repository conditions, although it is commonly encountered during metal plate production and welding processes. However, the main objective in this case is to evaluate microstructural transformations that may have an effect on the materials properties, or in the corrosion resistance of the alloy, through short-term thermal treatments. In a second phase of this program, additional studies at lower temperatures, closer to those prevailing on container surfaces during the containment period, will be conducted for extended times.

2 TECHNICAL BACKGROUND

As discussed below, very few studies exist in the literature on phase stability of alloy 825. However, it is accepted that alloy 825, a nickel-based alloy, is a metastable face-centered cubic (γ) material at room temperature. In the ternary Fe-Cr-Ni phase diagram at 400°C (Pugh and Nisbet, 1950), the chemical composition of alloy 825 (Table 2-1) corresponds to a location well within the γ-phase domain. As a consequence of its higher nickel content, it does not undergo a martensitic transformation upon fast quenching or cold working, as is the case of types 304L and 316L stainless steels, the other austenitic Fe-Cr-Ni alloys selected as candidate container materials. Also, no intermetallic phases have been identified in alloy 825, as in other high-nickel alloys containing chromium and molybdenum.

Table 2-1. Chemical composition in weight percent of alloy 825 (UNS N08825)

Source	C	Cr	Cu	Fe	Mo	Ni	Ti	Mn	S	Si	Al
Standard Specification [a]	0.05 [b]	19.5-23.5	1.5-3.0	22.0 [c]	3.0	38.0-46.0	0.6-1.2	1.0 [b]	0.03 [b]	0.5 [b]	0.2 [b]
Vendor Certificate [d]	0.010	22.09	1.79	30.41	3.21	41.06	0.82	0.35	<0.001	0.19	0.07
Independent Analysis	0.013	22.98	1.80	28.09	3.56	41.76	0.93	0.33	0.003	0.13	0.05

a — ASTM B424-92
b — Maximum
c — Minimum
d — INCO Alloys International Heat No. HH4371 FG

The most complete study on the thermal stability of alloy 825 was conducted by Raymond (1968). He found that when the alloy was thermally treated at temperatures ranging from 550 to 850°C, chromium-rich carbides precipitated at the grain boundaries. This is a well-known phenomenon for other austenitic Fe-Cr-Ni alloys, such as type 304 stainless steel. Precipitation of chromium-rich carbides, typically $M_{23}C_6$, is accompanied by chromium depletion along grain boundaries, leading to intergranular corrosion in different environments, a phenomenon called sensitization. The degree of sensitization increases significantly with the carbon content of the alloy and, to a lesser extent, with decreasing chromium content. A combination of low carbon content in the alloy with the addition of a carbide-forming alloying element, such as titanium, and the application of stabilizing heat treatments, is known to eliminate or at least attenuate chromium depletion (Gordon, 1977). This combined approach is used in the case of alloy 825. Nevertheless, chromium depletion and concurrent intergranular corrosion in specific environments occur under certain heat treatment conditions in terms of temperature and time.

Raymond (1968) studied the mechanism of sensitization and stabilization of alloy 825 by using transmission electron microscopy of jet-machined thin-foil samples and extraction-replica specimens. These techniques were used to study the morphology and distribution of the carbides. In addition, extracted carbide residues were analyzed by x-ray diffraction, x-ray emission spectrography, and wet chemical analysis to determine their chemical composition. Using this information, Raymond constructed

the time-temperature-precipitation diagram of alloy 825 in which a significant variation in the chemical composition of the carbides can be noted as a function of heat treatment temperature (650 to 1100°C) and time (0.1 to 10 h). The atomic ratio varied from 5Cr/84Ti to 43Cr/46Ti, whereas the primary carbide analysis of the initial solution-annealed (1200°C for 1 h) material corresponded to 3Cr/87Ti. The chromium content of the $M_{23}C_6$ precipitates was found to be directly correlated with the intergranular corrosion susceptibility of alloy 825 in boiling 65 percent nitric acid solution (Huey test), as represented in a time-temperature-sensitization (TTS) diagram. By comparing the precipitation morphology observed in alloy 825 with that of Inconel X-750, Raymond inferred that the higher chromium ratios correspond to a more pronounced chromium depletion down the grain boundaries, associated with a cellular, discontinuous mode of precipitation that tended to predominate at the lower end of the heat treatment range (up to 750°C).

Raymond concluded that alloy 825 should be stabilized against sensitization by heat treatments in the 930 to 980°C range, because the presence of titanium as a carbide-forming element, although useful, is not the primary factor preventing sensitization. Matrix diffusion of chromium is fast enough within that temperature range to eliminate chromium depletion. However, no direct evidence of chromium depletion or replenishment is presented in Raymond's paper since, at the time of its publication, the Analytical Electron Microscope (AEM) was unavailable. This instrument, which is a scanning transmission electron microscope (STEM) with energy dispersive x-ray spectroscopy capabilities, has been used extensively in recent years to determine chromium depletion profiles through areas across grain boundaries less than 100 nm wide in a variety of Fe-Cr-Ni alloys (Pande et al., 1977; Hall and Briant, 1984; Bruemmer et al., 1988; Was et al., 1981; Was and Kruger, 1985). However, no similar study has been conducted on alloy 825.

Brown (1969) indicated that evaluation of 15 different heats of alloy 825 with a nominal carbon content of about 0.03 weight percent resulted in a wide range of variation in susceptibility to intergranular corrosion in both boiling nitric acid and boiling ferric sulfate/sulfuric acid tests. He claimed that mill processing operations (intermediate working and annealing) may have a more pronounced effect on the resistance to sensitization than variations in composition within the nominal range. Although Brown pointed out that even materials from the same heat may exhibit widely different behaviors, he concluded that, in many cases, a stabilizing treatment at 930°C is beneficial. Nitric acid tests showed much larger differences in sensitization effects than the ferric sulfate tests, leading to the suggestion that submicroscopic σ phase (a Cr-rich, Ni-Fe-Cr-Mo intermetallic) may be involved in the enhanced susceptibility (Brown, 1969; Brown and Kirchner, 1973). This was originally proposed by Copson et al. (1961) for a material heat-treated at 649°C for 20 h, but the evidence supporting the presence of σ phase is inconclusive.

A study on the precipitation of particles in heat-treated alloy 825 using the Scanning Electron Microscope (SEM) has been recently published (Shaik et al., 1992). The authors identified three types of particles with different Cr/Ti ratios as intragranular precipitates already present in the mill-annealed condition. The particles could not be dissolved by solution treatment at 1200°C for 1 h, indicating that they are primary carbides formed from the solidification of ingots. Heat treatments at 870°C for times ranging from 1 to 264 h induced carbide precipitation at grain boundaries. Two types of carbide precipitates were identified. One was found to be composed mainly of chromium and molybdenum, with lower amounts of iron and nickel, while the second was less rich in chromium, but contained more iron and nickel and approximately the same percentage of molybdenum. Although aging time did not affect the composition of the precipitates, their size and density increased with time. The authors claimed that the nucleation of new particles did not cease even after 264 h aging. These results, however, have limited application

because the material used had an extremely high carbon content (0.09 weight percent), which is well beyond that specified for alloy 825 (see Table 2-1).

Alloy 825 should be expected to be unstable towards the topologically close packed (TCP) intermetallic σ phase. The presence of TCP phases in Ni-Cr-Mo alloys has been investigated extensively, and many semi-empirical correlations of σ-phase instability to alloy composition have been established to overcome the difficulty of developing thermodynamic phase diagrams for such complex alloys. The earliest of these attempts relied on the concepts of metallic bonding established by Linus Pauling (1938) and further developed by a number of investigators (Murphy et al., 1968; Barrows and Newkirk, 1972) for nickel-based alloys. The method essentially consists of assigning electron vacancy numbers, N_v, which correspond to unfilled d-band orbitals above the Fermi level, to each metallic element. The average N_v for an alloy is calculated on the basis of the atomic fraction of each alloying element and compared to a critical N_v^* value obtained from both empirical observations of a number of alloys and thermodynamic γ/σ phase boundaries for the ternary Ni-Cr-Mo system. Table 2-2 shows details of the calculation for the particular heat of alloy 825 examined in this study, assuming that titanium is fully dissolved in the matrix (solution-annealed condition). It can be seen that the calculated N_v value is equal to 2.44, whereas the critical N_v^* value for the Ni-Cr-Mo alloy system is equal to 2.32. Since the calculated N_v value is slightly above the critical one, the alloy is considered to be prone to σ-phase formation.

Table 2-2. Calculation of N_v and M_d values for the heat of alloy 825 used in this study

Alloying Element	Atomic Weight	Composition (wt %)	Composition (atomic fraction)	N_v [a]	M_d [b]
Cr	52.00	22.09	0.246	4.66	1.142
Mn	54.94	0.35	0.0035	3.66	0.957
Mo	95.94	3.21	0.0194	4.66	1.550
Ni	58.71	41.06	0.404	0.66	0.717
Fe	55.85	30.41	0.314	2.66	0.858
Ti	47.90	0.82	0.010	6.66	2.271
Si	28.09	0.19	0.004	6.66	1.900
Calculated values for alloy 825				2.44	0.904

a — Barrows and Newkirk, 1972
b — Morinaga et al., 1984

An alternative approach, proposed by Morinaga et al. (1984), can predict σ-phase stability for many alloy compositions over a wider range of temperatures. An average M_d value, which is the energy level of the d-bands in the alloy due to alloying additions, is calculated on the basis of the assigned M_d values for each alloying element and its atomic fraction in the alloy. The critical value for the formation of σ phase, M_d^*, is calculated using the following expression (Morinaga et al., 1984):

$$M_d^* = 0.834 + 6.25 \times 10^{-5}\ T\ (°K) \qquad (2\text{-}1)$$

The average M_d value for the heat of alloy 825 under study, as shown in Table 2-2, is slightly higher than the critical value of 0.898 calculated at 750°C by using Eq. (2-1). Both approaches gave essentially the same results, indicating that the heat of alloy 825 used in this study may be prone to σ-phase precipitation.

Although the discussion above indicates the possibility of σ-phase formation, the kinetics of this process is extremely sluggish, and very prolonged thermal treatments will be required at temperatures below 500°C.

3 EXPERIMENTAL PROCEDURES

For the determination of a TTS diagram for alloy 825, cubic samples of approximately 0.5 in. on each side were cut from a 0.5-in.-thick plate of the heat No. HH4371 FG supplied by INCO Alloys International in the hot-rolled and mill-annealed condition. The chemical composition of this heat, as provided by the manufacturer and determined by an independent laboratory, is given in Table 2-1, where the standard specification of alloy 825, according to the American Society for Testing and Materials (ASTM) Standard B 424-92, is also shown. The samples were mechanically polished, finishing with 200 grit SiC paper, and degreased with acetone.

The microstructure of the as-received material, to be identified in this report as mill-annealed (MA) samples, is shown at two magnifications in Figures 3-1 and 3-2. It is apparent from Figure 3-1 that the MA samples exhibit a dual grain size microstructure, with bands or areas of large grains surrounded by areas of very small grains. Two cuboidal precipitates of approximately the same size are seen in Figure 3-2. They are most probably titanium nitrides or titanium carbonitrides. In addition, the presence of a large number of small particles or precipitates, which are probably mixed titanium/chromium carbides, is clearly visible in some of the grains, while other grains are almost free of precipitates. It should be noted, however, that the grain boundaries are completely devoid of precipitates.

Since the MA samples exhibit a large number of small intragranular precipitates, which are probably carbides, half of the samples were solution-annealed at 1200°C for 10 min, followed by fast quenching in cold water, in order to dissolve the carbides. The microstructure of the resulting solution annealed (SA) samples is shown at two magnifications in Figures 3-3 and 3-4. It is apparent that the high-temperature treatment, although short, produces significant grain growth. Both micrographs reveal that the grain boundaries are free of precipitates and most of the intragranular precipitates, which are visible in Figure 3-2, are absent after solution annealing. The dissolution of the intragranular precipitates confirms that they are actually titanium/chromium carbides. However, the large cuboidal precipitates, which are clearly noticeable in Figure 3-2, were not dissolved by the high-temperature treatment, as is evident by comparing this figure with Figure 3-4, again suggesting that they may be titanium nitrides or carbonitrides.

Following the solution-annealing treatment, both MA and SA samples were heat treated at various temperatures ranging from 600 to 800°C for 0.1, 1.0, and 15.0 h. Heat treatments were conducted in a Lindberg tube furnace, using a quartz tube in which MA samples and SA samples were thermally treated simultaneously at the desired temperature. A very low air pressure of approximately 1.3×10^{-6} atm was maintained using a vacuum pump to limit the oxidation of the samples. A K-type (Chromel-alumel) thermocouple was introduced in a 1/16-in. borehole drilled in the SA sample to monitor the temperature accurately using a previously calibrated Doric Digitrend 235 data logger. Times ranging from 8 to 12 min were required to attain the desired temperature, as recorded from the instant at which the samples were introduced in the preheated furnace.

After completing the sequence of heat treatments, each cubic sample was cut in half using a water-cooled abrasive cut-off wheel in order to test duplicate specimens. The specimens were then wet-polished with 220 grit SiC paper, rinsed with double-deionized water, and then dried with an air blower. After measuring all dimensions with a calibrated caliper, the specimens were degreased with acetone, dried, and weighed in an analytical balance to the nearest 0.1 mg.

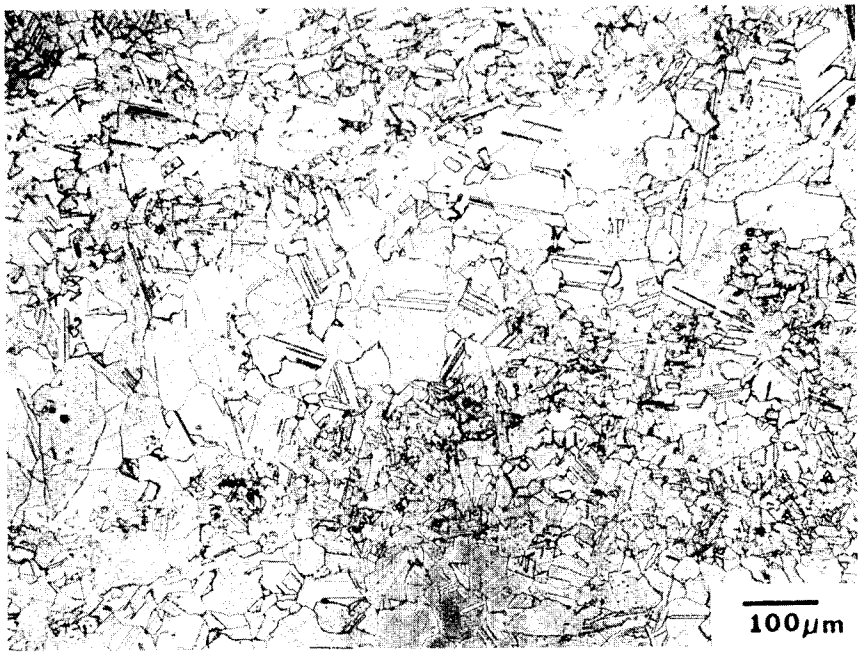

Figure 3-1. Microstructure of MA alloy 825 (transverse cross-section) at low magnification

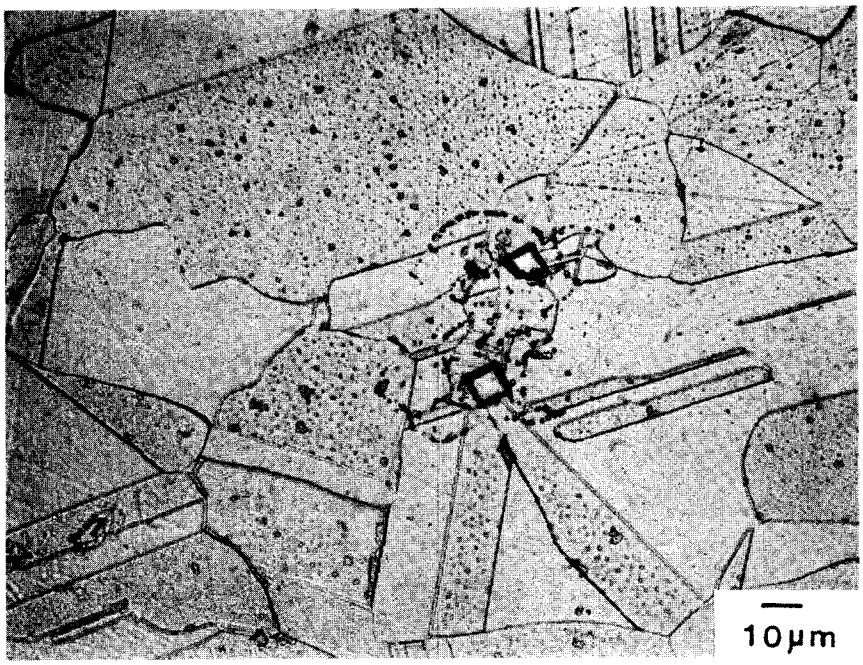

Figure 3-2. Microstructure of MA alloy 825 (transverse cross-section) at high magnification

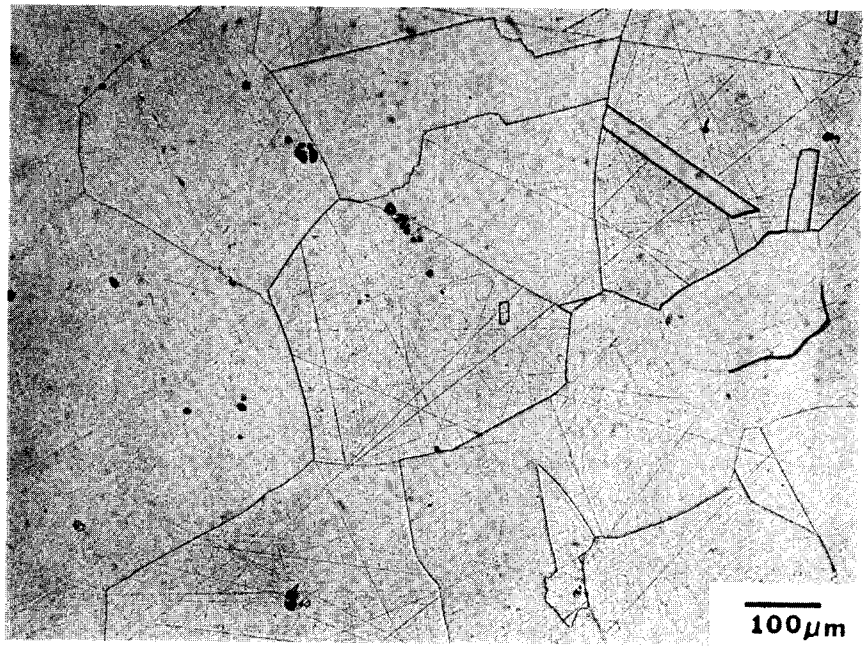

Figure 3-3. Microstructure of SA alloy 825 (transverse cross-section) at low magnification

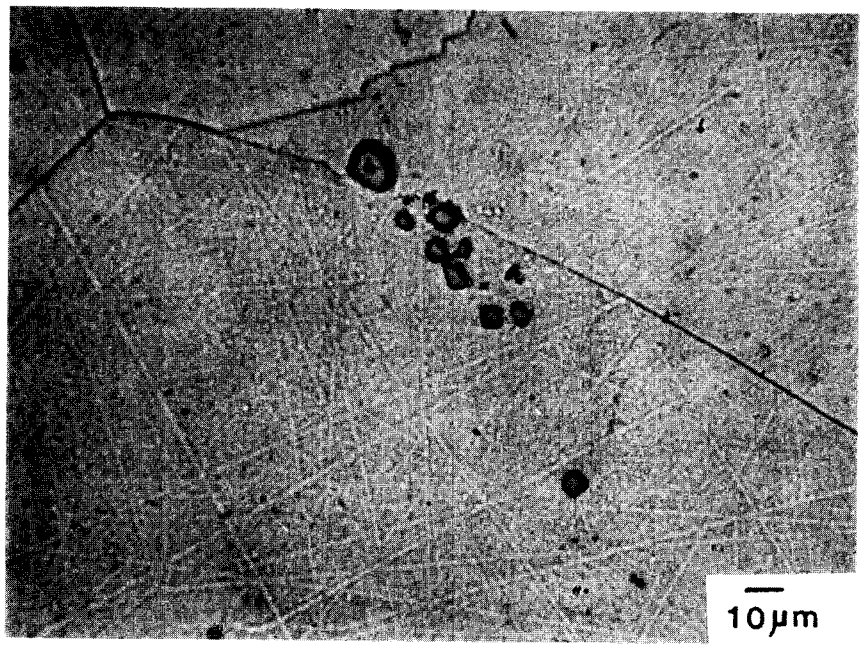

Figure 3-4. Microstructure of SA alloy 825 (transverse cross-section) at high magnification

The alloy 825 specimens were then exposed to boiling 65 percent nitric acid solution according to ASTM A-262-90, Standard Practice C (ASTM, 1991a) to detect their susceptibility to intergranular corrosion.

Exposures were conducted in 1000-ml Erlenmeyer flasks fitted with Allihn condensers using 450 ml of 65 $\pm$ 0.2 weight percent nitric acid solution, prepared with analytical reagent grade acid. Companion specimens, designated A and B, were simultaneously tested using a basket-shaped glass holder or glass cradle (ASTM, 1991b) in which the specimens were separated by a piece of microscope slide to avoid any contact. Solutions were heated and maintained at the boiling point on hot plates. Specimens were exposed, fully immersed into the boiling nitric acid solution, for a total of 240 h through five consecutive periods of 48 h each, the solution being replaced after each period. In some cases, as a result of test scheduling, the second period was shortened to 32 h, while the third one was extended to 64 h.

After each test period, the specimens were scrubbed with a nylon brush, washed with double-deionized water, rinsed with acetone, and then dried, prior to being weighed to the nearest 0.1 mg. When testing was completed, selected specimens were mounted for metallographic observation. Electrolytic etching in 5 percent nital was used to reveal grain boundaries, whereas carbide particles were detected by electrolytic etching in 80 percent phosphoric acid.

4 EXPERIMENTAL RESULTS

According to ASTM A-262-90, Standard Practice C, the evaluation of the susceptibility to intergranular corrosion is made by calculating an average corrosion rate over the five test periods. The corrosion rate is calculated as uniform dissolution or penetration, regardless of the localized morphology of the attack, by dividing the weight loss after each test period by the total surface area of the specimen, using the following expressions:

$$CR\ (mm/y) = 8.76 \times 10^4\ \Delta W / A \cdot t \cdot \delta \qquad (4\text{-}1)$$

and

$$cr\ (mg/dm^2 \cdot day) = 2.40 \times 10^6\ \Delta W / A \cdot t \qquad (4\text{-}2)$$

where ΔW is the weight loss in grams, A is the area in cm^2, t is the exposure time in hours and δ is the density, which is 8.14 g/cm^3 for alloy 825 (ASTM, 1991b).

Two methods were used to calculate average corrosion rates. In the first one, to be identified as Method 1, corrosion rates were calculated independently for each test period and an average value was obtained from the five exposure periods. In Method 2, corrosion rates were calculated at the end of the fifth period by taking into account the weight loss over the total exposure time from the beginning of the test.

A summary of the results obtained is presented in Tables 4-1 and 4-2 for MA and SA samples, respectively. For each heat treatment, the corrosion rates, given in mm/y or $mg/dm^2 \cdot day$ (mdd), represent an average of the rates for specimens A and B calculated independently by using the two methods described above. As expected, the two methods gave essentially the same results, indicating the absence of systematic errors in the determination of the corrosion rates. However, for the specimens with corrosion rates higher than 0.3 mm/y, it was noted that corrosion rates increased significantly after the initial exposure period of 48 h, reaching a maximum or a plateau in subsequent periods.

Figures 4-1 and 4-2 show the effect of heat treatment time at 700 and 750°C, respectively, on the corrosion rates calculated using Method 1 for MA and SA samples. These figures also illustrate the relatively minor differences in corrosion rates observed in most of the tests between companion specimens A and B, shown as different data points for each heat treatment condition. It is clearly seen in Figure 4-1 that the SA samples became far more sensitized than the MA samples after 15 h treatment at 700°C. However, at 750°C, only 1 h of heat treatment is required for SA samples to reach a relatively high corrosion rate, with a subsequent smaller increase in corrosion rate for 15 h treatment. The corrosion rate, nevertheless, was found to be the highest for the 700°C treatment. It is also apparent, from the results summarized in Table 4-1, that 0.1 h heat treatment of MA samples at any temperature is insufficient to produce a microstructure with a corrosion rate significantly higher than that of the original MA sample, since corrosion rates are lower than 0.13 mm/y for all these MA samples. It appears, however, that corrosion rates for the SA samples heat treated for 0.1 h are slightly higher than those of the corresponding MA samples, as seen by comparing the data from Tables 4-1 and 4-2. This observation is in agreement with the slightly greater corrosion rate exhibited by the SA sample without further heat treatment (0.12 mm/y) with respect to that of the original MA sample (0.10 mm/y).

Table 4-1. Average corrosion rates of MA specimens of alloy 825 after various heat treatments in boiling 65 percent HNO_3 acid (240 hours exposure)

Specimen	Temp (°C)	Time (h)	Corrosion Rate			
			(mm/year)		(mdd)	
			Method 1	Method 2	Method 1	Method 2
MA			0.107	0.109	23.9	24.4
MA*A1*T1	600	0.1	0.125	0.128	28.0	28.5
MA*A1*T2	600	1	0.138	0.142	30.8	31.7
MA*A1*T3	600	15	0.229	0.235	51.2	52.4
MA*A2*T1	638	0.1	0.101	0.102	22.6	22.6
MA*A2*T2	638	1	0.160	0.160	35.7	35.8
MA*A2*T3	638	15	1.029	1.029	229.5	229.5
MA*A3*T1	700	0.1	0.123	0.123	27.4	27.4
MA*A3*T2	700	1	0.177	0.177	39.5	39.5
MA*A3*T3	700	15	1.262	1.262	281.3	281.4
MA*A4*T1	750	0.1	0.128	0.128	28.5	28.5
MA*A4*T2	750	1	0.103	0.105	23.1	23.3
MA*A4*T3	750	15	1.125	1.153	250.8	257.1
MA*A5*T1	800	0.1	0.115	0.118	25.7	26.3
MA*A5*T2	800	1	0.132	0.136	29.3	30.3
MA*A5*T3	800	15	0.211	0.218	47.0	48.5
MA*A6*T1	900	0.1	0.110	0.110	24.5	24.5

Specimen identification: A1 . . . A6 and T1 . . . T3 indicate heat treatment temperatures and times, respectively.

Table 4-2. Average corrosion rates of SA specimens of alloy 825 after various heat treatments in boiling 65 percent HNO_3 acid (240 hours exposure)

Specimen	Temp (°C)	Time (h)	Corrosion Rate			
			(mm/year)		(mdd)	
			Method 1	Method 2	Method 1	Method 2
SA			0.116	0.118	25.9	26.1
SA*A1*T1	600	0.1	0.199	0.207	44.4	46.2
SA*A1*T2	600	1	0.107	0.107	23.9	23.9
SA*A1*T3	600	15	0.226	0.228	50.5	50.8
SA*A2*T1	638	0.1	0.120	0.120	26.7	26.8
SA*A2*T2	638	1	0.158	0.159	35.3	32.3
SA*A2*T3	638	15	1.397	1.397	311.5	311.4
SA*A3*T1	700	0.1	0.113	0.114	25.3	25.3
SA*A3*T2	700	1	0.341	0.341	76.0	76.1
SA*A3*T3	700	15	15.459	15.459	3447.6	3447.7
SA*A4*T1	750	0.1	0.127	0.128	28.4	28.5
SA*A4*T2	750	1	3.775	3.999	841.8	892.0
SA*A4*T3	750	15	4.937	5.059	1100.9	1123.1
SA*A5*T1	800	0.1	0.288	0.299	64.2	66.7
SA*A5*T2	800	1	0.533	0.533	118.9	119.0
SA*A5*T3	800	15	1.315	1.380	293.4	307.7
SA*A6*T1	900	0.1	0.173	0.173	38.5	38.5

Specimen identification: A1 . . . A6 and T1 . . . T3 indicate heat treatment temperatures and times, respectively.

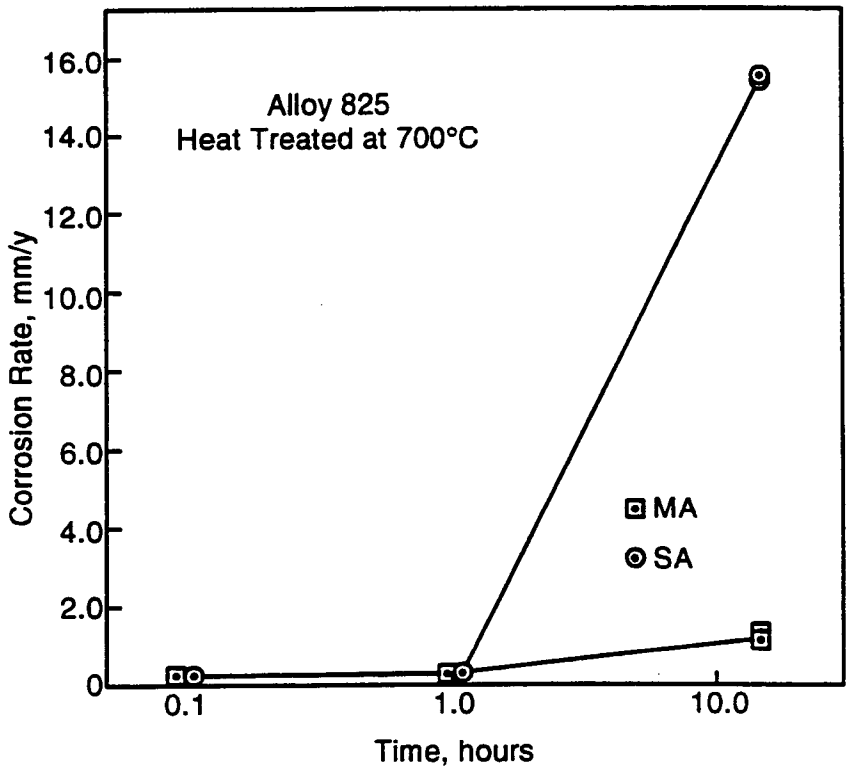

Figure 4-1. Corrosion rates for MA and SA samples of alloy 825 treated at 700°C as a function of heat treatment time

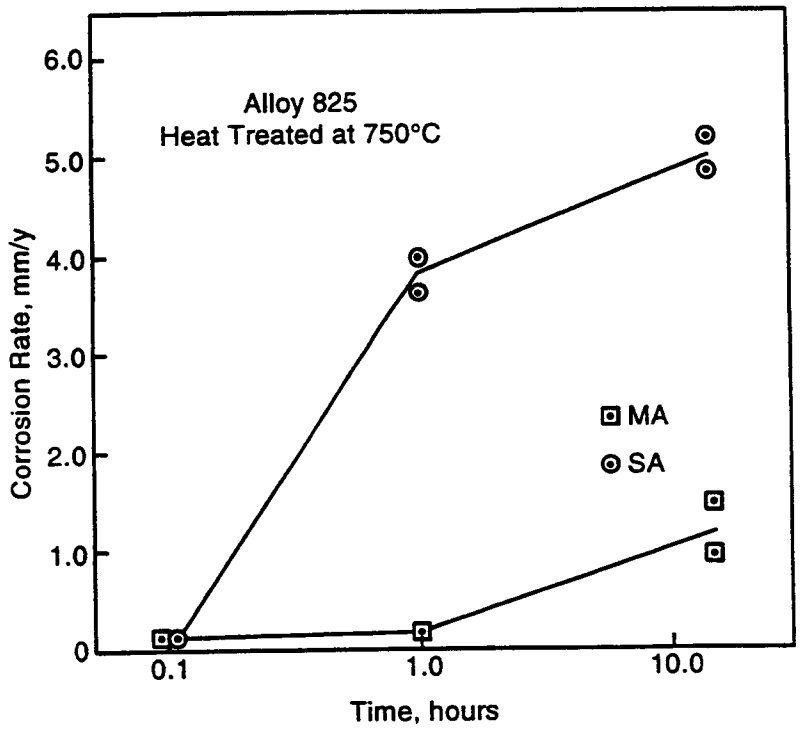

Figure 4-2. Corrosion rates for MA and SA samples of alloy 825 treated at 750°C as a function of heat treatment time

The corrosion rates summarized in Tables 4-1 and 4-2 for the heat-treated MA and SA samples are presented graphically in Figures 4-3 and 4-4, to illustrate the general trends in the effect of temperature and heat treatment time.

The results described above are expressed as corrosion rates in terms of uniform dissolution, following the procedures of the ASTM Standard. However, Figures 4-5 and 4-6 clearly show the development of localized dissolution along the grain boundaries, in the form of intergranular corrosion, for the heat-treated MA samples. It is noticeable in Figure 4-5 that intergranular penetration and the extent of the attack increased with increasing heat treatment time at 700°C, whereas the original MA sample only exhibited a very slight nonuniform attack. As shown in Figure 4-6, increasing the temperature to 750°C had a similar effect. At 800°C, however, the specimen surface exhibited a very irregular appearance, but with a limited amount of intergranular penetration. In agreement with the corrosion rate measurements, the heat-treated SA samples showed deep intergranular penetration, particularly for the samples heat treated for 15 h at temperatures of 700°C or above, as seen in Figures 4-7 and 4-8. No signs of localized attack are shown by the SA sample without additional thermal treatment (Figure 4-7a).

A convenient method for displaying the data of the intergranular corrosion tests is the use of TTS diagrams. The results described above are shown both for heat-treated MA and SA samples in Figure 4-9. A value of 0.3 mm/y has been adopted as a boundary between the sensitized and the nonsensitized regions of the diagram. Although this value can be considered arbitrary, it is the same as that adopted previously by Raymond (1968). It should be emphasized, however, that the location of the boundary depends on the solution composition and other environmental conditions that are fixed in the ASTM Standard. In a different environment, the sensitization domain may be reduced or extended beyond that shown in Figure 4-9.

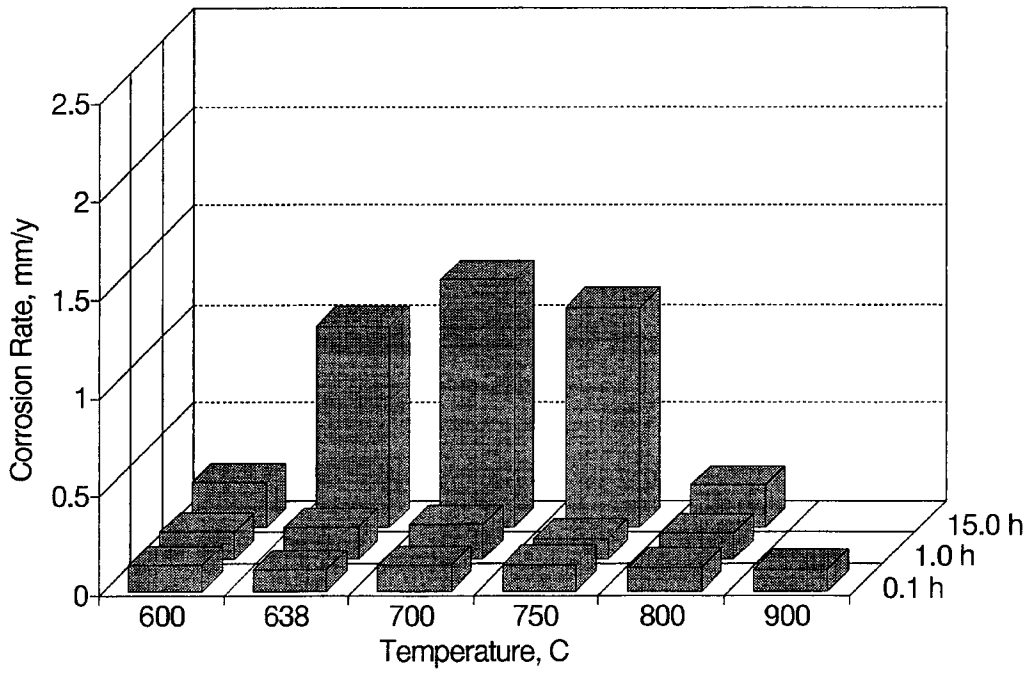

Figure 4-3. Effect of heat treatment temperature and time on the corrosion rate of MA samples of alloy 825

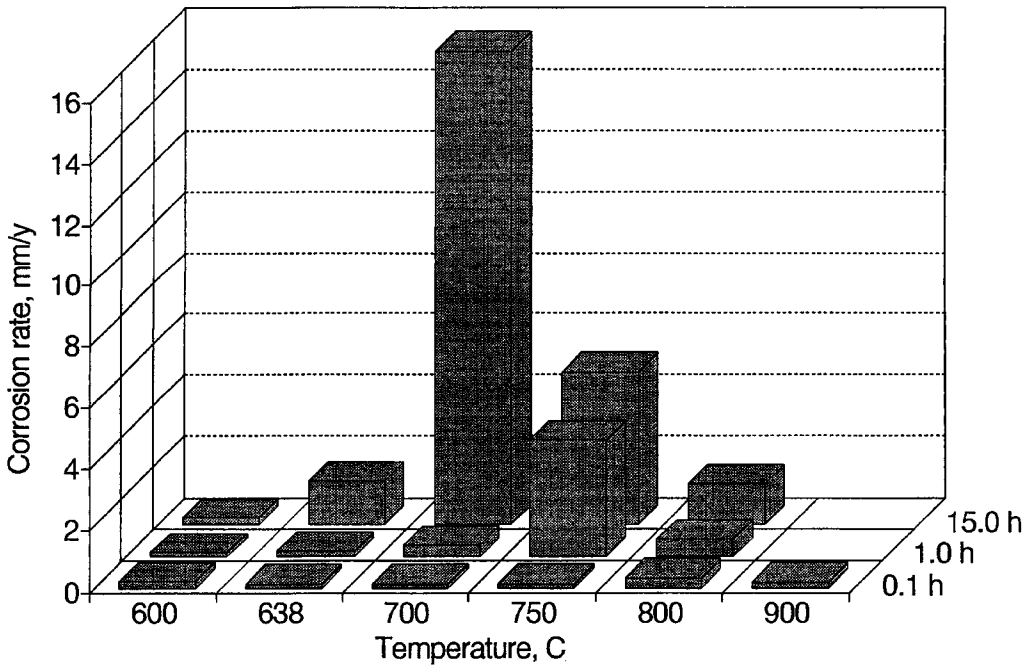

Figure 4-4. Effect of heat treatment temperature and time on the corrosion rate of SA samples of alloy 825

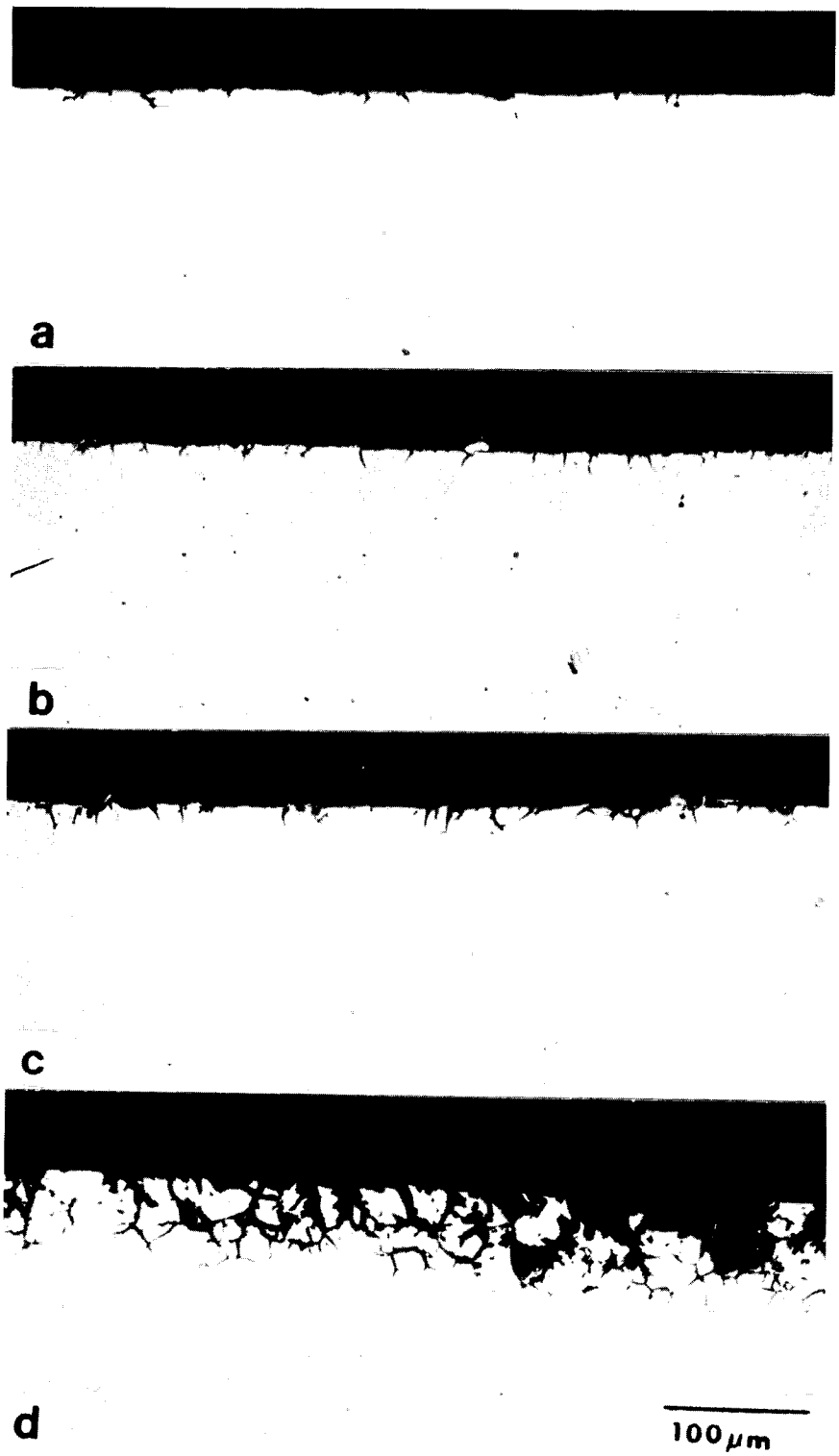

Figure 4-5. Micrographs showing the intergranular attack on heat treated MA samples of alloy 825. (a) MA; (b) MA + 700°C/0.1 h; (c) MA + 700°C/1.0 h; (d) MA + 700°C/15 h.

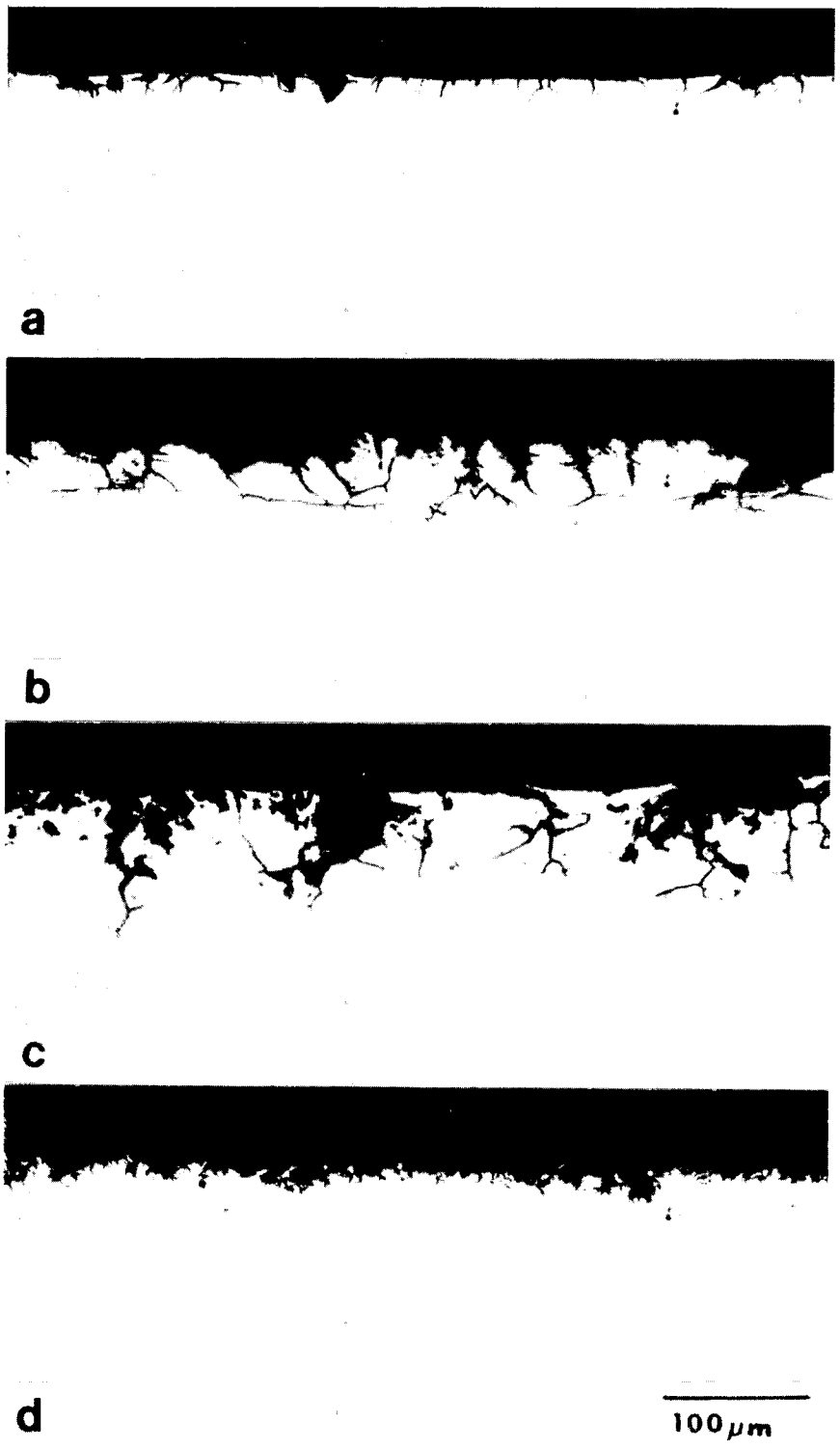

Figure 4-6. Micrographs showing the intergranular attack on MA samples of alloy 825 heat treated for 15 h at various temperatures. (a) 600°C; (b) 638°C; (c) 750°C; (d) 800°C.

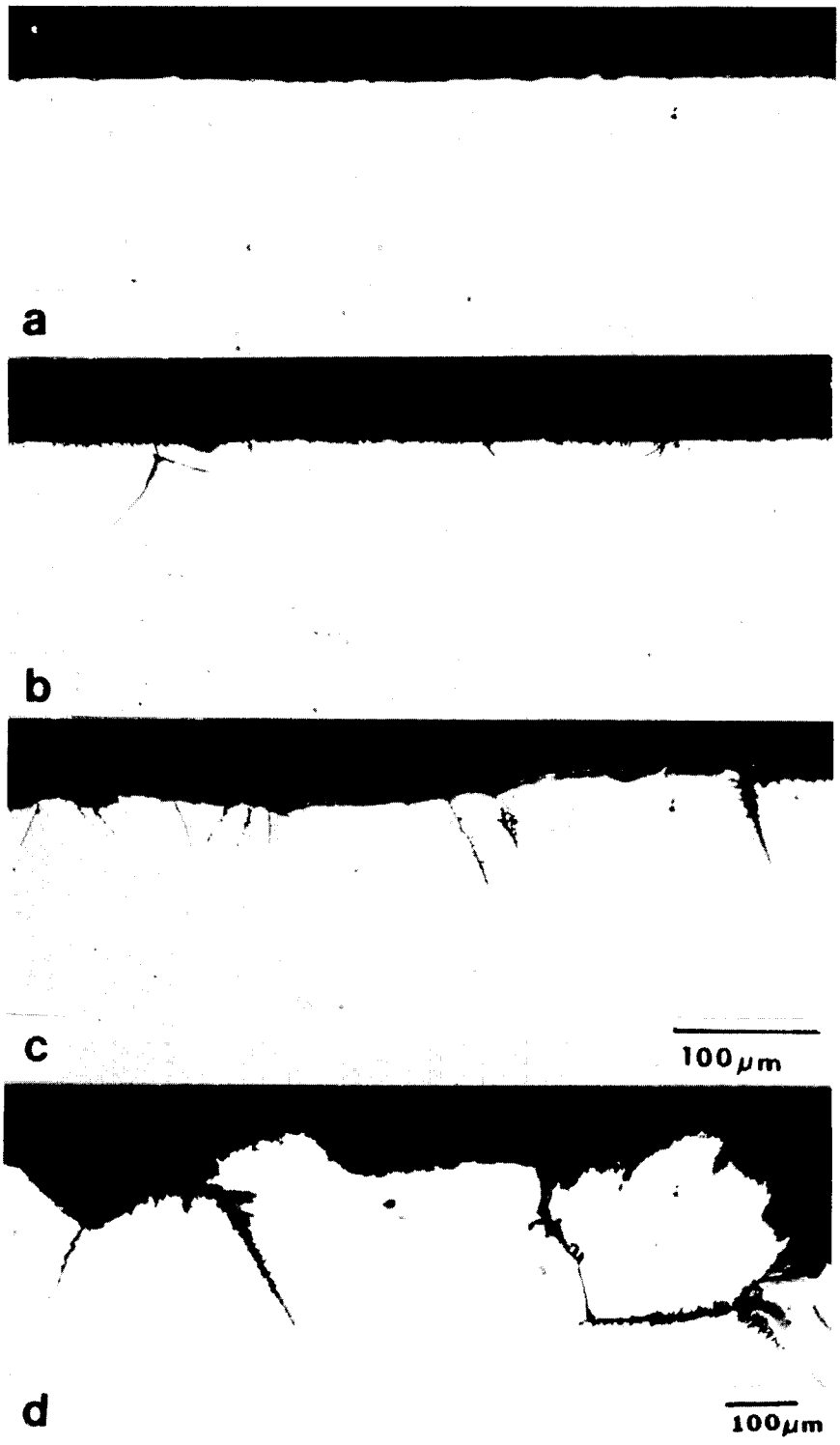

Figure 4-7. Micrographs showing the intergranular attack on heat treated SA samples of alloy 825. (a) SA; (b) SA + 700°C/0.1 h; (c) SA + 700°C/1.0 h; (d) SA + 700°C/15 h.

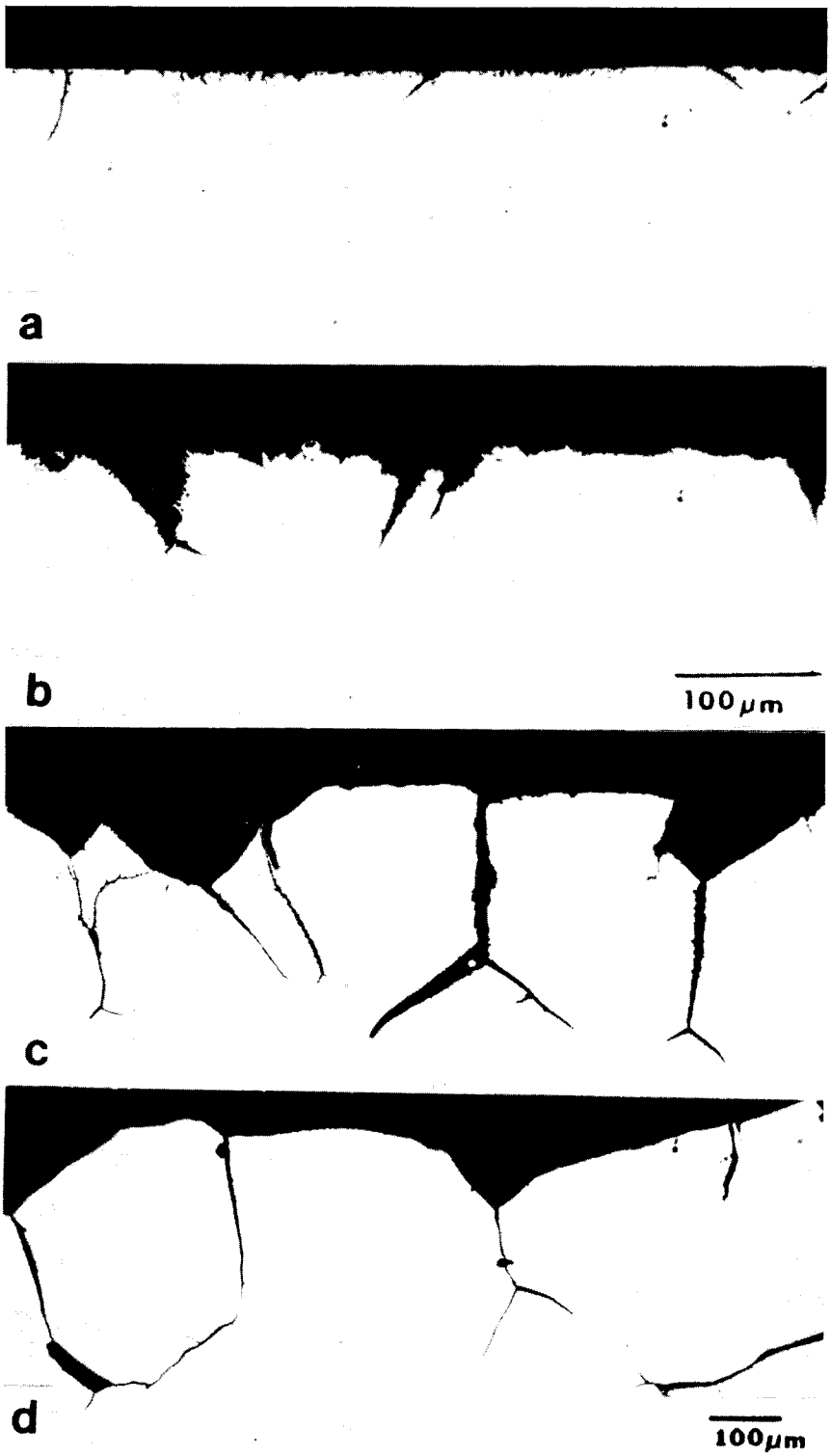

Figure 4-8. Micrographs showing the intergranular attack on SA samples of alloy 825 heat treated for 15 h at various temperatures. (a) 600°C; (b) 638°C; (c) 750°C; (d) 800°C.

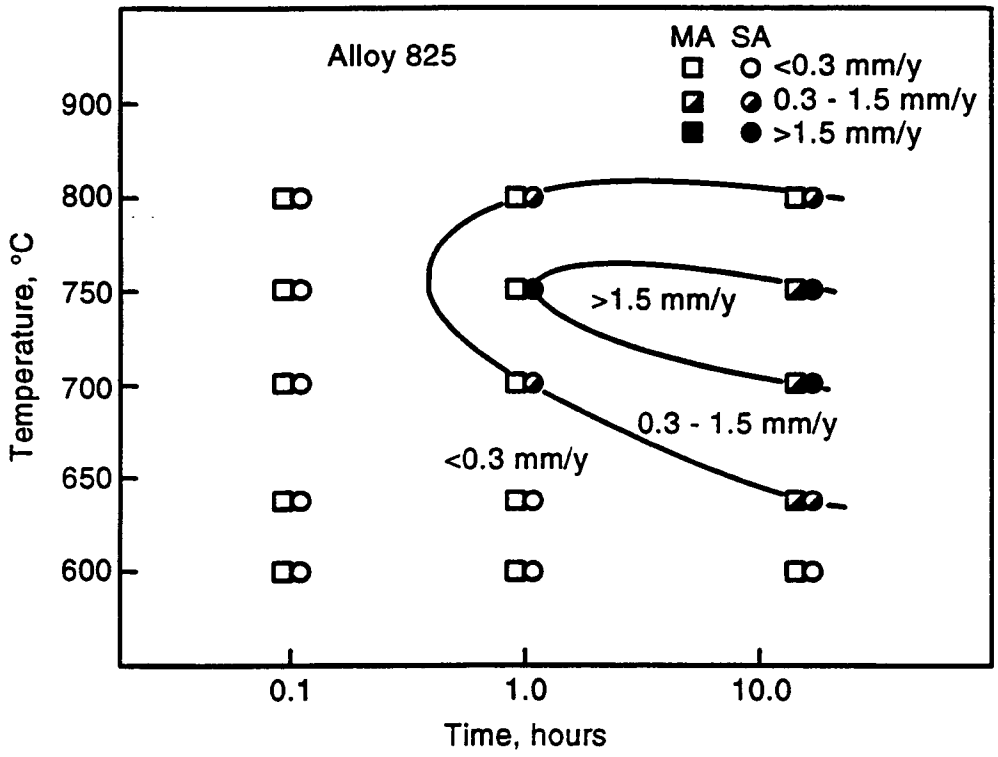

Figure 4-9. TTS diagram for MA and SA samples of alloy 825 in boiling 65 percent nitric acid solution

5 DISCUSSION

The results described in the previous section essentially confirm the findings reported by Raymond (1968) regarding the temperature range for sensitization and the location of the "nose" in the TTS diagram for alloy 825. However, as shown in Figure 5-1, for a material solution-annealed at 1204°C, and in Figure 5-2, for that annealed at 940°C for 1 h (temperature of the current stabilizing treatment for mill-annealed samples), Raymond (1968) found much larger sensitization domains, in terms of time and temperature, than that plotted in Figure 4-9. In addition, it should be noted that, in the present work, a corrosion rate as high as 15.5 mm/y was attained in SA samples after 15 h of heat treatment at 700°C, whereas Figure 5-1 shows that approximately the same rate was obtained by Raymond (1968) after just 0.2 h.

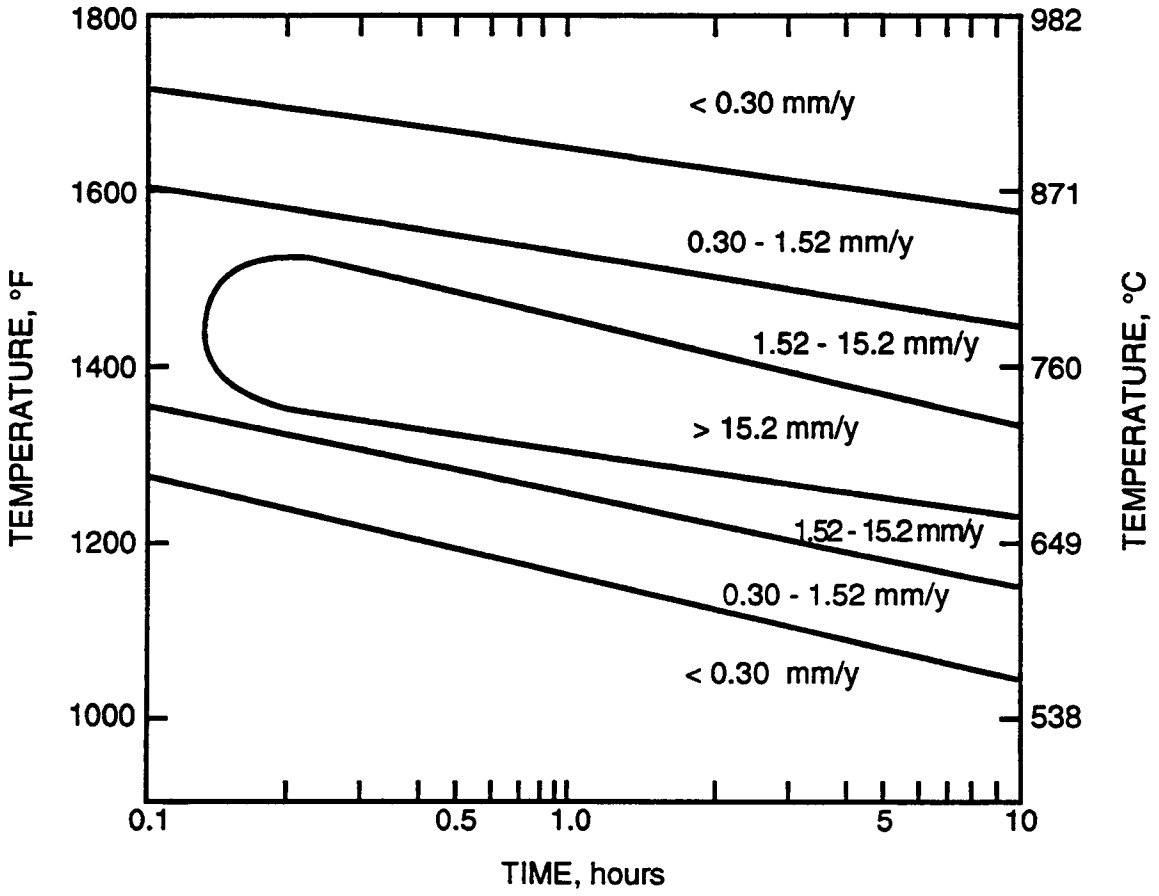

Figure 5-1. TTS diagram for alloy 825 (C: 0.03 weight percent) in boiling 65 percent nitric acid solution after annealing at 1204°C for 1 h (after Raymond, 1968).

The simplest explanation for the greater degree of sensitization of the material studied by Raymond (1968) is related to the higher carbon content. Raymond (1968) tested a heat of alloy 825 with a carbon content of 0.03 weight percent, whereas the heat used in the present study contains only 0.01 weight percent. The effect of the higher carbon content on the sensitization of alloy 825 is understandable in terms of chromium depletion. Chromium carbides precipitate initially along grain boundaries at sensitization

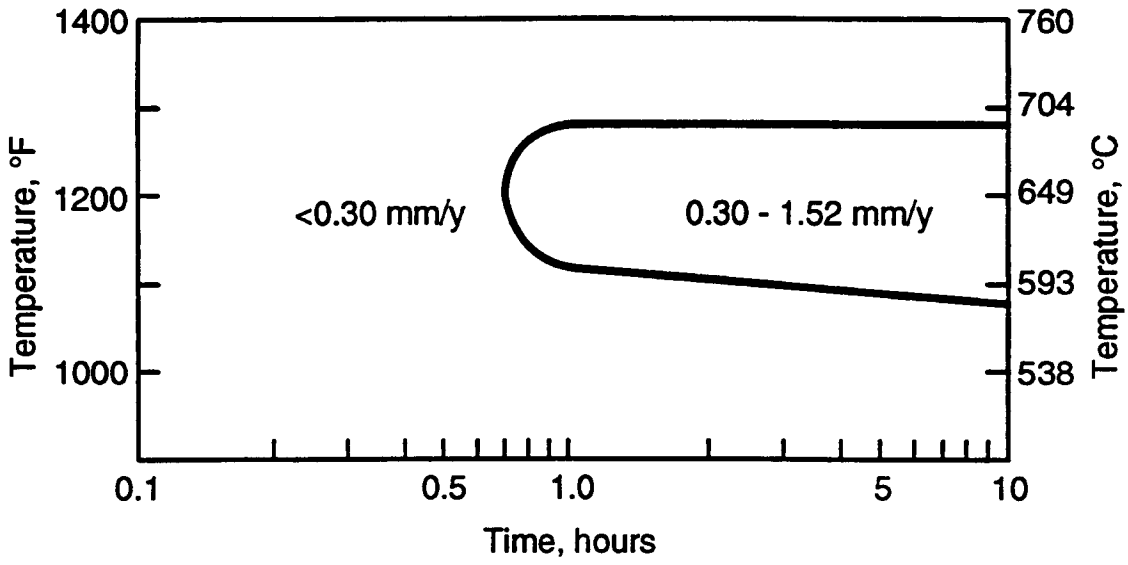

Figure 5-2. TTS diagram for alloy 825 (C: 0.03 weight percent) in boiling 65 percent nitric acid solution after annealing at 940°C for 1 h (after Raymond, 1968)

temperatures because the solubility of carbon in alloy 825 is about 0.01 weight percent (Raymond, 1968). This is the value measured at about 980°C, but it could be even slightly smaller at lower temperatures.

The precipitation of chromium-rich carbides is accompanied by chromium depletion of the regions adjacent to the boundaries to levels well below those in the matrix. Carbon diffuses interstitially toward the grain boundary quite readily, but the substitutional diffusion of chromium from the matrix to the depleted region is too slow to permit replenishment in a relatively short time. Most of the models developed for chromium depletion (Stawström and Hillert, 1969; Was and Kruger, 1985; Bruemmer, 1990) postulate that a local equilibrium is established at the carbide/matrix interface as

$$M_{23}C_6 \rightleftharpoons 23\ M + 6\ C \qquad (5\text{-}1)$$

where it is assumed that M is mostly Cr, in the case of alloy 825 (Raymond, 1968). Therefore, a higher carbon content in the alloy implies a lower chromium activity or concentration at the interface, which also decreases with decreasing temperature. Whereas the chromium concentration at the carbide/matrix interface is thermodynamically determined, the profile of the chromium concentration gradient is dominated by diffusional factors. As a consequence, a more extended depleted region corresponding to a lower chromium concentration at the interface will result if all the other influential factors, such as alloy composition, time, and temperature, are maintained constant.

The sequence in the carbide precipitation for the SA samples heat treated at 700°C is shown in Figures 5-3 through 5-5. In Figure 5-3, no precipitates are present along grain boundaries after 0.1 h of heat treatment. After 1 h (Figure 5-4), partial precipitation is noted along some grain boundaries, while there are boundaries completely decorated with carbides after 15 h treatment, as shown in Figure 5-5, although the precipitation is not necessarily extended to all grain boundaries. On the other hand, a treatment at 600°C for 15 h is not prolonged enough to induce carbide precipitation, as shown in Figure 5-6.

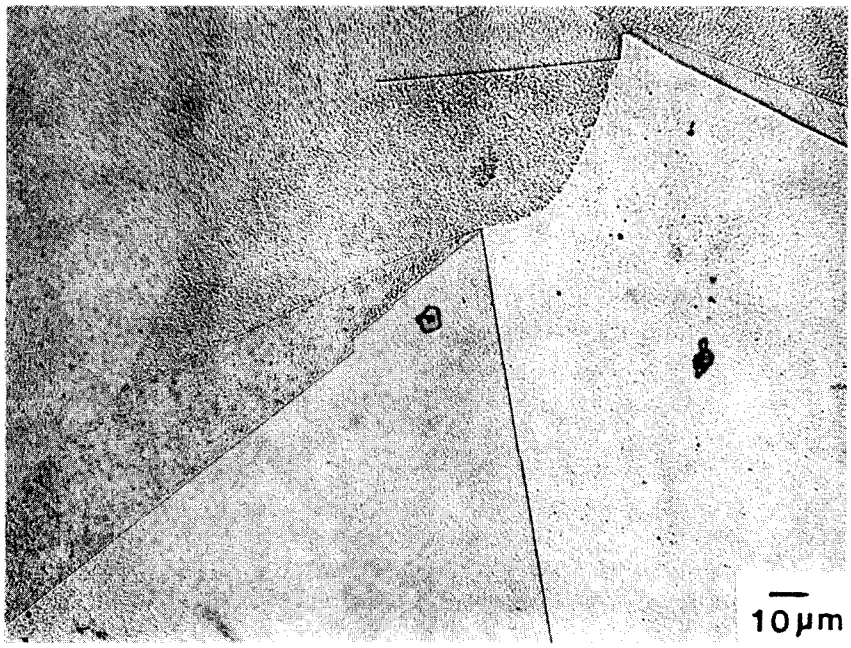

Figure 5-3. Micrograph of SA alloy 825 heat treated at 700°C for 0.1 h

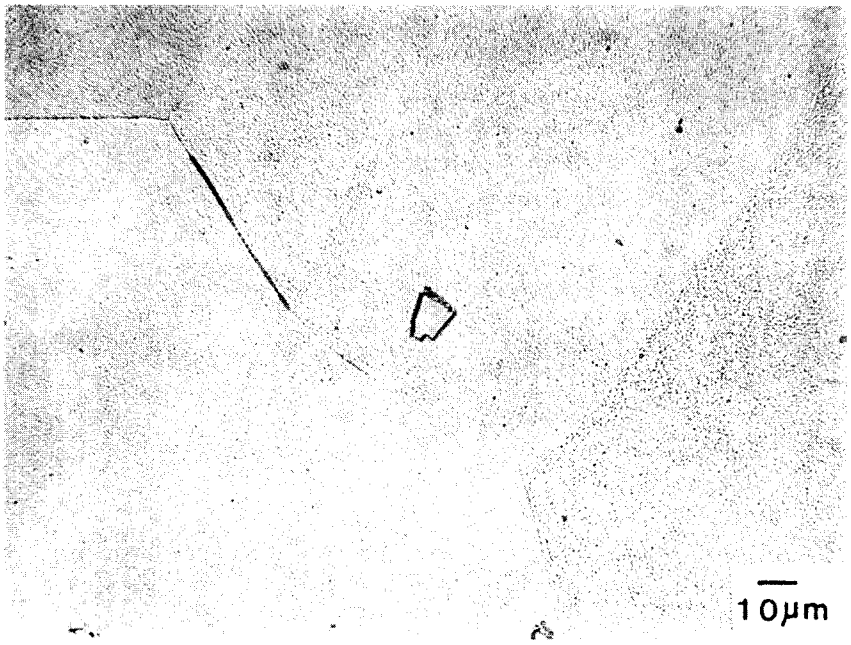

Figure 5-4. Micrograph of SA alloy 825 heat treated at 700°C for 1.0 h

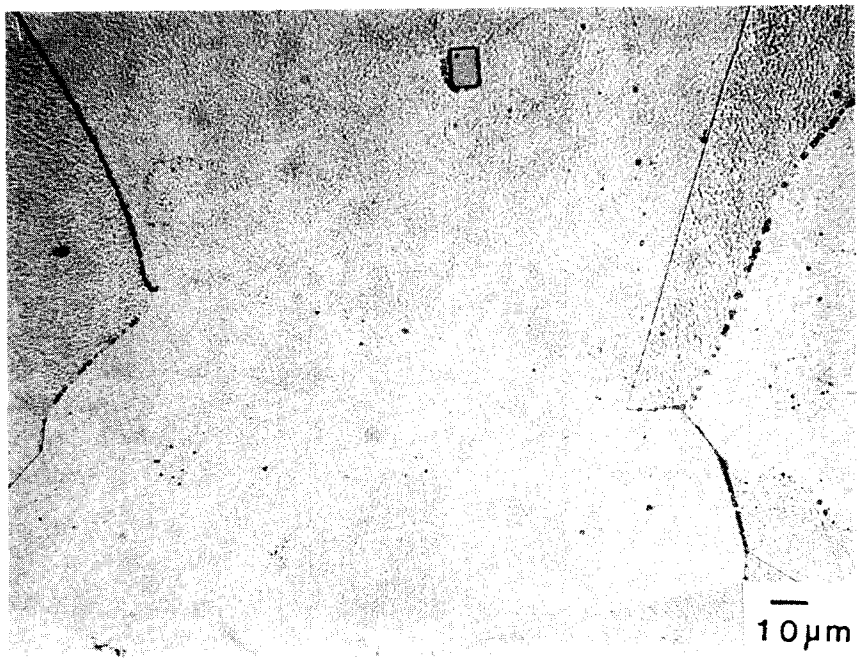

Figure 5-5. Micrograph of SA alloy 825 heat treated at 700°C for 15 h

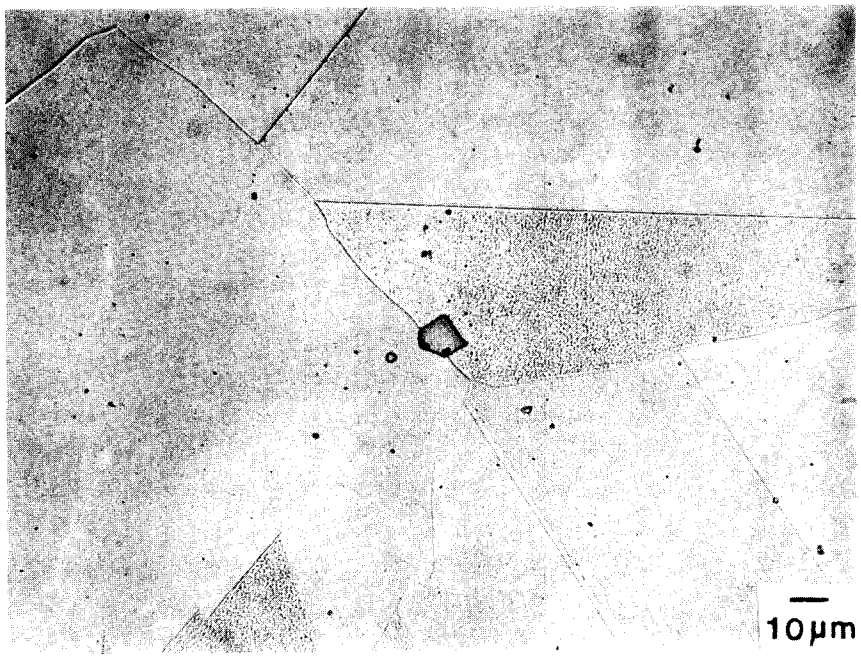

Figure 5-6. Micrograph of SA alloy 825 heat treated at 600°C for 15 h

The significantly lower degree of sensitization of the heat-treated MA samples, as compared to that of the SA samples, can also be explained with the arguments above. Since the MA material contains a relatively large number of intragranular carbide particles, there is far less carbon in solid solution available for precipitation at grain boundaries during subsequent heat treatment in the 600 to 800°C range. The result is equivalent to that expected for a material with a low carbon content. The comparison of Figure 5-7 with Figure 5-8 clearly illustrates that, for the MA samples, 15 h are required to attain an almost continuous precipitation along grain boundaries. Figure 5-7 shows mostly intragranular carbide precipitation with almost a complete absence of intergranular carbides.

The decrease in the corrosion rate that is observed for samples heat treated for 15 h at temperatures above 700°C is also understandable in terms of the chromium-depletion theory. At increasingly higher temperatures, the rate of diffusion of chromium becomes high enough to replenish, at least partially, the chromium-depleted regions, and, therefore, sensitization decreases, although carbides are still precipitated and they can even grow in grain boundaries. This is illustrated by comparing Figure 5-9 with Figure 5-10, where it is noticeable that the increase in temperature leads to a coarsening of the carbide particles precipitated along the boundaries. A similar effect was noted on MA samples heat treated at 800°C for 15 h, which leads to a very irregular appearance of the surface without a significant intergranular penetration after exposure to boiling nitric acid (Figure 4-6d). Such irregular morphology results from a shallow intergranular attack of all grain boundaries in the small grain-sized material and the attack of localized areas surrounding intragranular carbides. It can also be expected that, at any temperature, desensitization will occur after a heat treatment prolonged enough to replenish completely the chromium-depleted area, even though the carbides may be still precipitated and undergoing restructuring and growth to form more discrete particles. This is a plausible explanation for the decrease in corrosion rate with increasing heat treatment time from 0.2 to 10 h at 760°C, which is apparent in Raymond's results depicted in Figure 5-1.

One of the important observations in this work is that, despite the decrease in carbon content down to 0.01 weight percent and the optimization of the stabilization treatment by annealing at 940°C, alloy 825 is still prone to sensitization when heat treated in the 600 to 800°C range. Hence, it may be susceptible to intergranular corrosion after prolonged exposure to an appropriate environment, which can be far less aggressive than boiling nitric acid.

In order to evaluate potential sensitization effects at lower temperatures, corrosion rates measured in SA samples heat treated for 15 h at temperatures ranging from 600 to 700°C were plotted on a logarithmic scale as a function of the reciprocal of the heat treatment temperature, as shown in Figure 5-11. A typical Arrhenius behavior was observed with an apparent activation energy of approximately 292.6 kJ/mole (69.9 kcal/mole). This value is relatively close to the activation energy for matrix diffusion of chromium in a nickel-based alloy such as alloy 600 (Ni-15%Cr-6%Fe), in which a value of 277.7 kJ/mole has been measured by Pruthi et al., 1977. Data for binary Ni-Cr alloys, reported also by Pruthi et al., indicate that the activation energy increases with increasing chromium content, reaching about 290.4 kJ/mole for Ni-29.7%Cr. This effect of the chromium content on the activation energy for chromium diffusion may be the reason of the high value for the activation energy obtained in the present study, since the chromium content of alloy 825 is higher than that of alloy 600. It appears that the corrosion rates measured in the thermally-treated SA samples can be related, at least qualitatively, to the degree of sensitization, as given by the level of chromium depletion and the width of the depleted zone. The width of the depleted zone is approximately given by $2(Dt)^{1/2}$, where D is the matrix diffusion coefficient of chromium at the temperature of interest and t is time. A detailed experimental study of chromium-depletion profiles in alloy 825, as affected by heat treatment temperature and time, would be

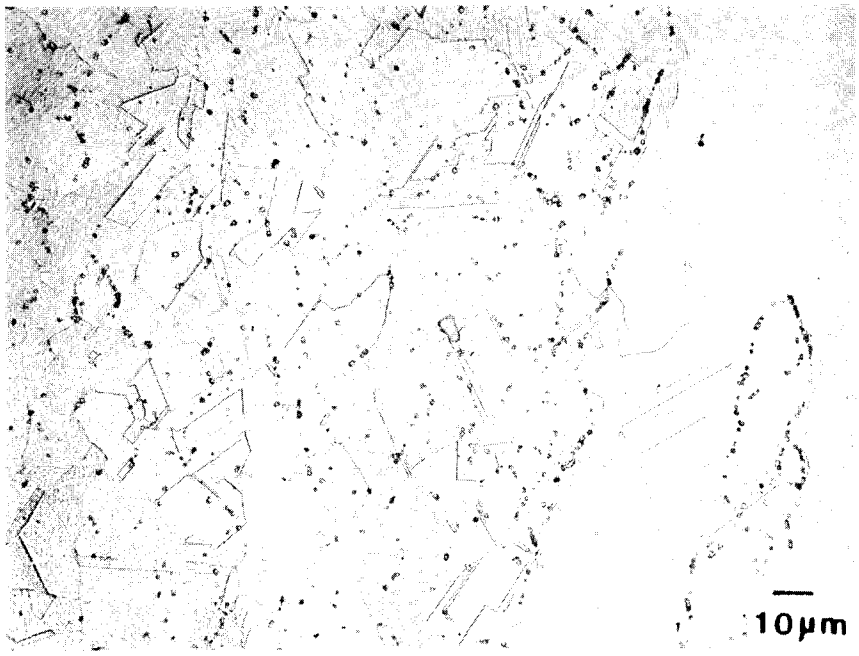

Figure 5-7. Micrograph of MA alloy 825 heat treated at 700°C for 1.0 h

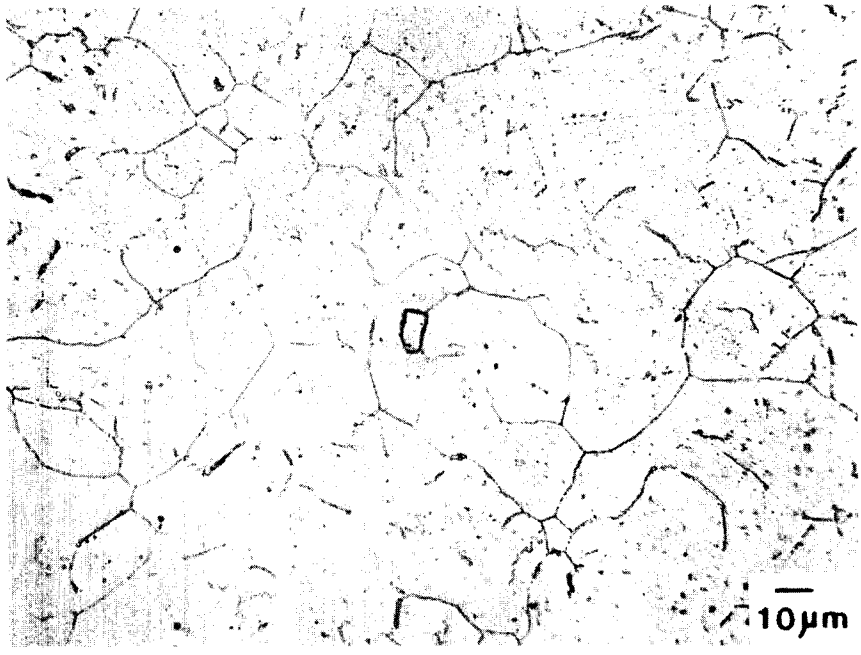

Figure 5-8. Micrograph of MA alloy 825 heat treated at 700°C for 15 h

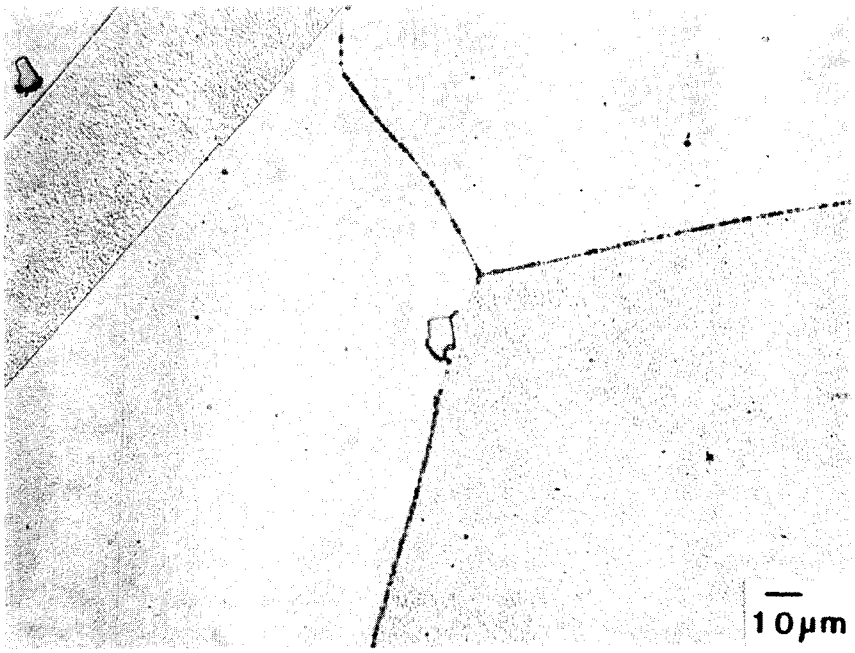

Figure 5-9. Micrograph of SA alloy 825 heat treated at 750°C for 15 h

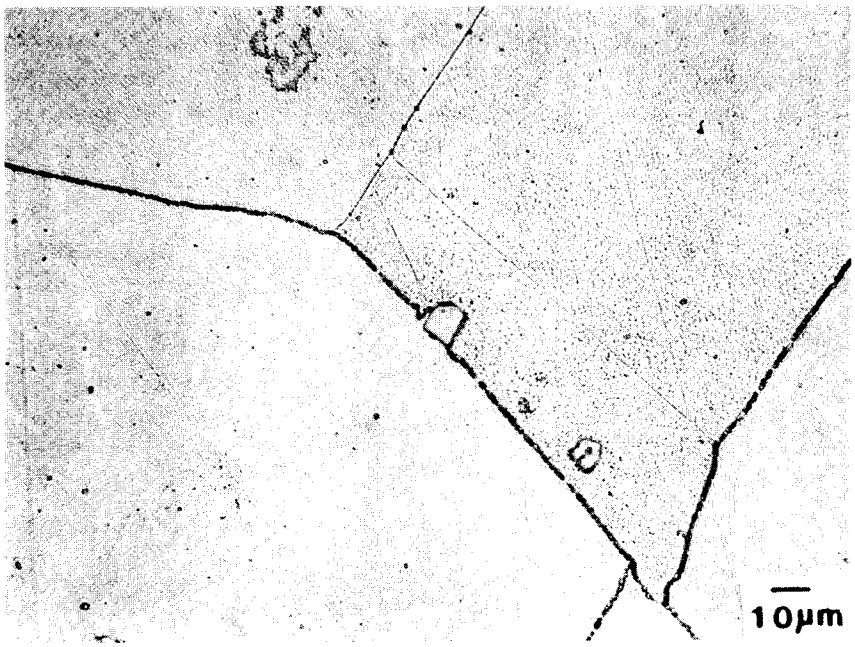

Figure 5-10. Micrograph of SA alloy 825 heat treated at 800°C for 15 h

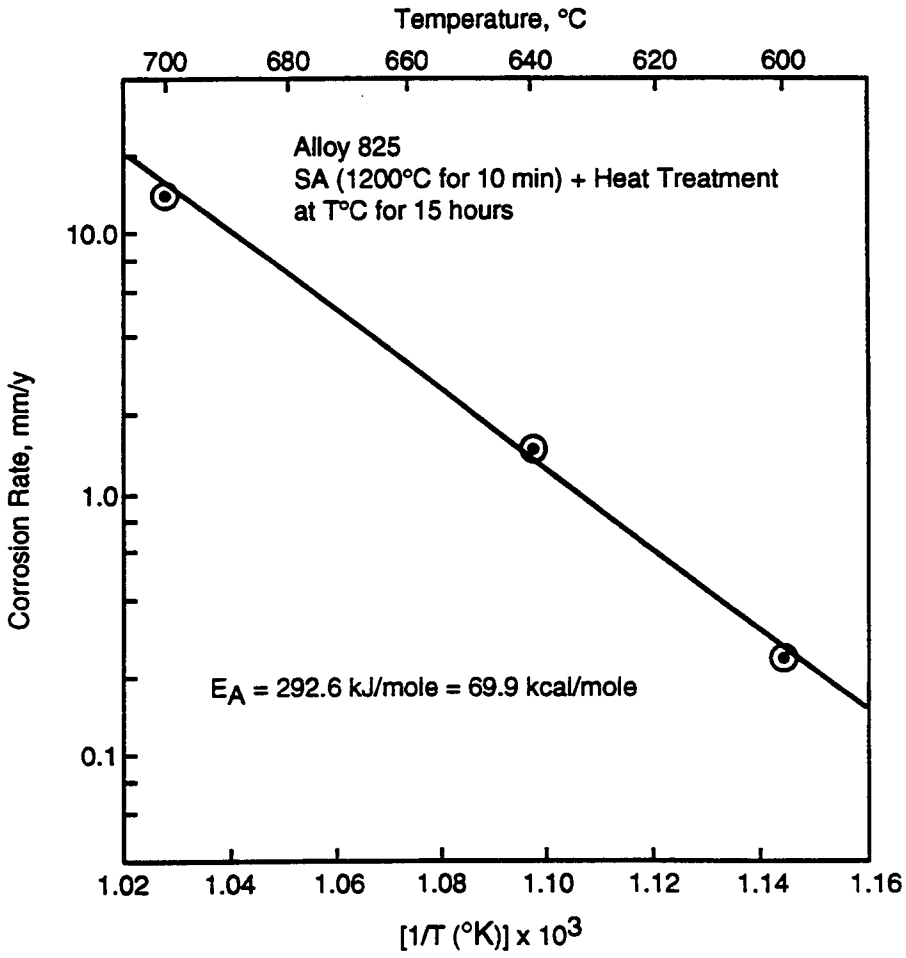

Figure 5-11. Corrosion rates for SA samples of alloy 825 in boiling 65 percent nitric acid solution as a function of the reciprocal of the heat treatment temperature

required to confirm that suggestion, coupled with the application of thermodynamic and kinetics models for the interpretation of chromium depletion.

Leaving aside any mechanistic interpretation of the activation energy values discussed above, it is apparent, however, that such high values indicate a very strong temperature dependence. A decrease in temperature from 600 to 400°C implies a decrease of at least five orders of magnitude in the rate of the controlling process (i.e., chromium diffusion) if there is no change in the mechanism with respect to that prevailing in the 600 to 700°C range. This implies that heat treatments extended for more than 18 years will be required at 400°C to obtain the degree of sensitization observed in the high temperature range. In order to study the thermal stability of alloy 825 at temperatures closer to those expected under repository conditions within a realistic time frame, it would be necessary to enhance metallurgical processes responsible for sensitization, such as carbide precipitation and chromium diffusion, among others. This can be accomplished by introducing a higher dislocation density in the γ matrix of SA samples through cold work prior to the sensitization treatments. It is known that cold work (up to 20 percent) prior to sensitization increases significantly the degree of sensitization of type 304 stainless steel (Pednekar and Smialowska, 1980). However, cold working of austenitic stainless steels results in the

formation of martensite, which is not the case of alloy 825. This is an additional incentive to evaluate the influence of cold work on the low-temperature behavior of alloy 825, because the effect cannot be predicted simply by comparing with that of stainless steels. The effect of cold work on thermal stability is also important from a practical point of view. Surface and near-surface areas of containers could be affected by cold work effects arising from unwanted sudden mechanical loads, impingement by wall-rock shear offsets, and other interactions leading to localized plastic deformation.

This study shows that the ASTM A 262-90 Standard Practice C can be used for assessing quantitatively the degree of sensitization of alloy 825. However, a simpler and less time-consuming test is desirable. Electrochemical methods, such as the electrochemical potentiokinetic reactivation (EPR) test method (Clarke, 1981), have been developed and used in the last fifteen years for detecting and evaluating the degree of sensitization of type 304 and other austenitic stainless steels. The origin of the EPR method can be traced to the study of sensitization in alloy 600, conducted by Duffaut et al. (1966). Although it is used far less for nickel-base alloys than for austenitic stainless steels, the anodic polarization behavior during reverse potential scanning in a sulfuric acid solution containing KSCN as an activator is a suitable approach for detecting sensitization. More recently, the EPR method has been applied successfully to the determination of TTS diagrams for alloy 800 (Fe-33%Ni-22%Cr) heat treated for 10 to 1000 h at temperatures ranging from 525 to 600°C (Mignone et al., 1982). Test conditions should be optimized to apply this method to alloy 825, mainly because the presence of titanium and molybdenum as alloying elements may introduce significant differences in the anodic polarization response.

It is important, in this context, to clarify certain additional differences between the boiling nitric acid test (commonly known as the Huey test) and the EPR test method. For annealed austenitic stainless steels in boiling 65 percent nitric acid solution, the open circuit potential lies in the range 1.0 to 1.2 V_{SHE} (Cowan and Tedmon, 1973). Under such strong oxidizing conditions, it is considered, as discussed by Cowan and Tedmon among others, that chromium carbides and σ phase precipitated along grain boundaries may be selectively attacked, in addition to chromium-depleted regions. On the other hand, Bruemmer et al. (1988) demonstrated that, under the mildly oxidizing conditions prevailing in the EPR test (potentials lower than 0.2 V_{SHE}), only chromium-depleted regions (with chromium contents below $\approx$ 13.5 weight percent) are selectively dissolved in austenitic stainless steels. In this study, sensitization of alloy 825 was evaluated only in boiling nitric acid. Because it was observed in a material with a low carbon content (0.01 weight percent), the possible presence of σ phase and its contribution to grain boundary dissolution needs to be ascertained and examined further.

6 SUMMARY AND CONCLUSIONS

The results of this study clearly indicate that alloy 825, despite the low carbon content attained with new production methods and the introduction of an appropriate stabilization treatment, is still susceptible to sensitization. Hence, intergranular corrosion becomes possible under specific environmental conditions if the alloy is thermally treated in the 600 to 800°C range for a time period sufficient to precipitate chromium-rich carbides at grain boundaries.

As expected, solution annealing, prior to those thermal treatments, enhanced significantly the degree of sensitization, leading to high corrosion rates in the boiling 65 percent nitric acid solution. The present work confirms the temperature range of sensitization and the nose temperature of the TTS diagram reported by Raymond (1968). It is also shown that the decrease in carbon content from 0.03 weight percent to the current 0.01 weight percent, although it increases the heat treatment time required for sensitization, does not suppress this detrimental phenomenon. Less than 30 min heating at 750°C is sufficient to induce sensitization in SA materials.

The sensitization process was found to be strongly dependent on temperature, with an apparent activation energy of approximately 292 kJ/mole (70 kcal/mole) in the 600 to 750°C range, which indicates that very prolonged heat treatment times may be required to induce sensitization at lower temperatures. For predictions of long-term stability of alloy 825 under repository conditions, it will be necessary to conduct heat treatments in the 400 to 600°C range to be able to proceed with reliable extrapolations into the temperature range of interest which is below 250°C. It should be noted, however, that a decrease in temperature from 600 to 400°C implies a decrease of more than five orders of magnitude in the controlling process rate if there is no change in the mechanism with respect to the higher temperature regime studied in this work. Heat treatment times of at least 18 years will be required to attain an experimentally detectable degree of sensitization at 400°C. It can be concluded that cold working should be used as a plausible accelerating factor to study the low-temperature sensitization propensity of alloy 825, also taking into consideration that containers emplaced in the repository may be cold-worked locally in a variety of ways, including impingement of rocks and accidental handling forces.

A preliminary analysis of the propensity to σ-phase formation based on metallic bonding concepts, using the N_v or the M_d approach, indicates that grain boundary precipitation of σ phase is possible for the composition of alloy 825 under study. This needs further examination because a stabilized microstructure may not prevent precipitation, although this process could be extremely slow at temperatures ranging from 400 to 600°C.

A final conclusion of this work relates to the testing methods for sensitization. Although it was found that boiling nitric acid was an appropriate medium to evaluate susceptibility to intergranular corrosion, it is highly desirable to apply a less time-consuming technique. The optimization or modification of the EPR method seems to be justifiable as a next step for the detection and evaluation of sensitization in alloy 825.

7 REFERENCES

ASTM. 1991b. Standard test methods of detecting susceptibility to intergranular attack in wrought, nickel-rich, chromium-bearing alloys. G 28-85. Philadelphia, PA: ASTM. *Annual Book of Standards*. 03.02:91-95.

ASTM. 1991a. Standard practices for detecting susceptibility to intergranular attack in austenitic stainless steel. A 262-90. Philadelphia, PA: ASTM: *Annual Book of Standards*. 03.02:1-18.

Barrows, R.G., and J.B. Newkirk. 1972. A modified system for predicting σ formation. *Metallurgical Transactions* 3A(11):2889-2893.

Brown, M.H. 1969. The relationship of heat treatment to the corrosion resistance of stainless alloys. *Corrosion* 25(10):438-443.

Brown, M.H., and R.W. Kirchner. 1973. Sensitization of wrought high nickel alloys. *Corrosion* 29(12):470-474.

Bruemmer, S.M. 1990. Quantitative modeling of sensitization development in austenitic stainless steel. *Corrosion* 46(9):698-709.

Bruemmer, S.M., L.A. Charlot, and B.W. Arey. 1988. Sensitization development in austenitic stainless steel: Correlation between STEM-EDS and EPR measurements. *Corrosion* 44(6):328-333.

Clarke, W.L. 1981. *The EPR Method for the Detection of Sensitization in Stainless Steels*. NUREG/CR-1095. Washington, DC: NRC.

Copson, H.R., B.E. Hopkinson, and F.S. Lang. 1961. Behavior of Ni-O-Nel nickel-iron-chromium alloys in intergranular corrosion evaluation tests. *Proceedings ASTM*. Philadelphia, PA: ASTM: 61:879-889.

Cowan II, R.L., and C.S. Tedmon Jr. 1973. Intergranular corrosion of iron-nickel-chromium alloys. M.G. Fontana and R.W. Staehle, eds. *Advances in Corrosion Science and Technology*. Plenum Press, New York. 3:293-400.

Duffaut, F., J.P. Pouzet, and P. Lacombe. 1966. Potentiostatic study of structural modifications caused in a Ni-Cr-Fe alloy by heat treatment at 650°C. *Corrosion Science* 6:83-85.

Gordon, G.M. 1977. Physical metallurgy of Fe-Cr-Ni alloys. R.W. Staehle, J. Hochmann, R.D. McCright, and J.E. Slater, eds. *Stress Corrosion Cracking and Hydrogen Embrittlement of Iron Base Alloys*. Houston, Texas: National Association of Corrosion Engineers (NACE): 893-945.

Hall, E.L., and C.L. Briant. 1984. Chromium depletion in the vicinity of carbides in sensitized austenitic stainless steels. *Metallurgical Transactions* 15A(5): 793-811.

McCright, R.D. 1988. *An Annotated History of Container Candidate Material Selection*. UCID-21474. Livermore, CA: Lawrence Livermore National Laboratory (LLNL).

McCright, R.D., W.G. Halsey, G.E. Gdowski, and W.L. Clarke. 1991. Candidate container materials for Yucca Mountain waste package designs. *Proceedings Nuclear Waste Packaging Focus '91*. La Grange Park, IL: ANS: 125-135.

Mignone, A., A. Borello, and A. La Barbera. 1982. The electrochemical potentiokinetic reactivation method — An analysis of different treatments of experimental data. *Corrosion* 38(7):390-402.

Morinaga, M., N. Yukawa, H. Adachi, and H. Ezaki. 1984. New PHACOMP and its applications to alloy design. *Superalloys Source Book*. Materials Park, OH: ASM International.

Murphy, H.J., C.T. Sims, and A.M. Beltran. 1968. PHACOMP revisited. *Journal of Metals* 20(12):46-54.

Pande, C.S., M. Suenaga, B. Vyas, H.S. Isaacs, and D.F. Harling. 1977. Direct evidence of chromium depletion near the grain boundaries in sensitized stainless steels. *Scripta Metallurgica* 11(8): 681-684.

Pauling, L. 1938. The nature of interatomic forces in metals. *Physical Review* 54(12):899

Pednekar, S., and S. Smialowska. 1980. The effect of prior cold work on the degree of sensitization in type 304 stainless steel. *Corrosion* 36(10):565-577.

Pruthi, D.D., M.S. Anand, and R.P. Agarwala. 1977. Diffusion of chromium in Inconel 600. *Journal of Nuclear Materials* 64:206-210.

Pugh, J.W., and J.D. Nisbet. 1950. A study of the iron-chromium-nickel ternary system. Transactions of the American Institute of Mining and Metallurgical Engineers. *Journal of Metals* 188:268-276.

Raymond, E.L. 1968. Mechanisms of sensitization, and stabilization of Incoloy nickel-iron-chromium alloy 825. *Corrosion* 24(6):180-188.

Shaik, M.A., M. Iqbal, M. Ahmad, J.I. Akhtar, and K.A. Shoaib. 1992. Precipitation study of heat-treated Incoloy 825 by scanning electron microscopy. *Journal of Materials Science Letters* 11:1009-1011.

Short, D.W., D.J. Ruffner, and L.J. Jardine. 1991. Engineered barrier system and waste package design concepts for a potential geologic repository at Yucca Mountain. *Proceedings Nuclear Waste Packaging Focus '91*. La Grange Park, IL: ANS:113-124.

Stahl, D. 1992. Source term concept and definition. *Presentation to Nuclear Waste Technical Review Board*. Las Vegas, NV. October 14-16.

Stawström, C., and M. Hillert. 1969. An improved depleted-zone theory of intergranular corrosion of 18-8 stainless steel. *Journal of the Iron and Steel Institute* 207(1):77-85.

Was, G.S., and R.M. Kruger. 1985. A thermodynamic and kinetic basis for understanding chromium depletion in Ni-Cr-Fe alloys. *Acta Metallurgica* 33(5):841-854.

Was, G.S., H.H. Tischner, and R.M. Latanision. 1981. The influence of thermal treatment on the chemistry and structure of grain boundaries in Inconel 600. *Metallurgical Transactions* 12A(9):1397-1408.